Neuro-Oncology
27(12), 3132–3144, 2025 | https://doi.org/10.1093/neuonc/noaf187 | Advance Access date 9 August 2025

STAT3 expression in brain metastases from breast cancer is correlated with molecular subtype and impacts clinical outcome

Alessia Pellerino[†], Neibla Priego[†,¶], Luca Bertero, Alessia Andrea Ricci, Luca Mangherini, Francesco Bruno, Alessandra Beano, Gloria Mittica, Marinella Mistrangelo, Diego Garbossa, Joaquim Bosch-Barrera[¶], Paola Cassoni, RENACER, Manuel Valiente[¶], Riccardo Soffietti[‡], and Roberta Rudà[‡]

All author affiliations are listed at the end of the article
[†]These authors equally contributed to this work.
[‡]Co-senior authors.

[¶]Spanish National Network on Brain Metastases (RENACER)

Corresponding Author: Alessia Pellerino, MD, PhD, Division of Neuro-Oncology, Department of Neuroscience "Rita Levi Montalcini," University and City of Health and Science Hospital, Turin 10126, Italy (alessia.pellerino@unito.it).

Abstract

Background. A high pSTAT3 expression in reactive astrocytes surrounding brain metastases (BrM) promotes tumor growth in preclinical models. The impact of STAT3 expression on outcome of patients with BrM from breast cancer is unknown.

Methods. The expression of pSTAT3 in reactive astrocytes of 100 resected BrM from breast cancer was investigated by immunohistochemistry and correlated with molecular subtypes, risk of intracranial recurrence and progression-free survival. To explore whether clinical findings could be replicated in preclinical models, we used two human BrM cell lines (triple-negative MDA231 and HER2-positive HCC1954-), and evaluated pSTAT3 expression on established BrM.

Results. High pSTAT3 expression in reactive astrocytes was detected in 57% of BrM, and prevailed in triple-negative (80.9%) over HER2-positive (43.2%) and luminal (33.3%) metastases ($P = .002$). A different pSTAT3 expression was confirmed in animal models: as it was detected in 50% of reactive astrocytes in triple-negative MDA231 BrM lesions compared with 13% in HER2-positive HCC1954—BrM lesions ($P = .0001$). Patients with high pSTAT3 expression in BrM displayed higher intracranial recurrence rate (66.7 vs 33.3%) ($P = .0353$), and shorter intracranial PFS (9 months vs 28 months) ($P = .0002$), and this finding was significant for triple-negative patients only ($P = .0008$).

Conclusions. This study indicates that STAT3 expression prevails in reactive astrocytes surrounding triple-negative BrM in comparison to HER2-positive and luminal BrM, and these findings mirror those observed in animal models. A high STAT3 expression correlates with higher risk of intracranial recurrence and shorter progression-free survival, particularly in patients with triple-negative BrM.

Key points

- High STAT3 expression in reactive astrocytes prevails in triple negative BrM (TNBrM).
- Two BrM animal models confirm that STAT3 expression differs across molecular subtypes of BC.
- High STAT3 expression predicts risk of recurrence, shorter i-PFS, especially in TNBrM.

Importance of the Study

The results of this study demonstrate that the expression of STAT3 in reactive astrocytes surrounding brain metastases should be considered as a biomarker of prognostic significance across the different molecular subtypes of breast cancer. Thus, a close monitoring with MRI of patients who underwent surgical resection of brain metastasis with high STAT3 expression may be suggested. The prominence of STAT3 expression in reactive astrocytes in triple-negative brain metastases suggests as well that targeting STAT3 is attractive for patients with triple-negative breast cancer for whom effective therapies are still lacking.

Brain metastasis (BrM) is a complication of metastatic breast cancer (MBC), accounting for 10%-30% of patients, with impairment in cognitive function, quality of life, and poor prognosis.[1] The risk of development of BrM in BC depends on several factors, such as age, performance status, systemic disease stage at diagnosis, and molecular subtype.[2–6] Molecular profile influences the outcome: according to a meta-analysis on MBC 15% of hormone receptor (HR)-positive patients, 31% of epidermal growth factor receptor 2 (HER2)-positive patients, and 32% of triple-negative breast cancer (TNBC) patients develop BrM.[1] Although advances in targeted therapy have improved the control of extracranial disease, the efficacy of anticancer agents on BrM is limited,[7] except for anti-HER2 drugs, such as tucatinib and trastuzumab deruxtecan.[8]

The highly specialized brain microenvironment plays a major role in inducing a selective pressure on BrM initiating cells, consisting in the selection of additional genomic and epigenomic alterations, that allow them to adapt.[9] Reactive astrocytes are a key component of microenvironment, that surrounds BrM, and favor the co-option of a pro-metastatic program between metastatic cells and local immunosurveillance.[10] In this regard, Priego et al.[11] described a subpopulation of peritumoral reactive astrocytes, located at the periphery of BrM, that induce the signal transducer and activator of transcription 3 (STAT3) pathway and promotes a pro-metastatic microenvironment by modulating both the innate and acquired immune system.[12] The overexpression of STAT3 in reactive astrocytes has a negative effect on the activation of CD8 +T cells,[13] resulting in a local immunosuppression mediated by TIMP1, that favors BrM progression. Moreover, highly infiltrative BrM exhibit abundant STAT3 expression.[14]

Priego et al.[11] investigated STAT3 expression in reactive astrocytes of 91 resected human BrM from non-small-cell lung cancer (NSCLC), BC, melanoma and other primary tumors, and observed that 89% were positive for STAT3 in reactive astrocytes, with a variability in signal intensity. The overall survival (OS) from diagnosis of BrM was available for 39 patients and high STAT3 expression was associated with a worse OS (10 months) as compared with low STAT3 expression (18 months).

The aim of this manuscript is to evaluate in a large cohort of patients with BrM from MBC, who were completely resected, the expression of pSTAT3 in reactive astrocytes of peritumoral tissue across different molecular subtypes, and to correlate with risk of brain recurrence and intracranial progression-free survival.

Patients and Methods

Eligibility Criteria

Eligible patients were retrospectively identified from the biobank of the Pathology Unit of University of Turin and Spanish National BrM Network (RENACER) from January 2021 to April 2023. Inclusion criteria were as follow: ≥18 years of age; histological diagnosis of BrM from BC; complete surgical resection of BrM; resection including 5-10 mm of normal tissue beyond the BrM margins to identify and evaluate the presence of reactive astrocytes; single or multiple BrM that did not receive previous radiosurgery or whole-brain radiotherapy (WBRT). Conversely, previous cytotoxic chemotherapy and/or hormonal therapies and/or targeted therapies for the treatment of primary tumor and/or extracranial metastases were allowed. Exclusion criteria were as follows: incomplete surgical resection of BrM; surgery for BrM previously treated with any type of radiotherapy; absence or inadequate amount of peritumoral tissue surrounding BrM; coexistence of dural and/or leptomeningeal dissemination; incomplete follow-up data or survival <3 months. Histological, molecular, and clinical data, as well as outcome measures, were retrieved by chart review. Clinical characteristics, such as age, sex, systemic disease status, Karnofsky performance status (KPS) at the time of diagnosis of BrM, number and location of BrM, adjuvant radiotherapy and/or chemotherapy and/or targeted therapies for BrM following surgery, presence and type of recurrence, and intracranial progression-free survival (i-PFS) were analyzed. Due to the short follow-up of the cohort (2021-2023) OS data were collected but not analyzed.

The study was approved by the local IRB "Comitato Etico Interaziendale—A.O.U. Città della Salute e della Scienza di Torino" (N. 364/2022—0107665) in accordance with the guidelines of the Declaration of Helsinki. The need for informed consent was waived by the competent regulatory authorities due to the retrospective nature of the study. RENACER samples were in compliance with protocols approved by the Institutional Review Board (IRB) (CEI PI 25_2020-3) and informed consent was signed by each patient.

Brain Metastasis Samples and Immunohistochemistry

Sections with 3 or 4 μm of thickness were obtained from a formalin-fixed paraffin-embedded (FFPE) tissue block of

each case and stained with hematoxylin and eosin (H&E) or submitted to immunohistochemistry (IHC) and FISH analysis. Breast cancer predictive and prognostic markers were assessed on BrMs according to ASCO/CAP criteria 2020, 2018/2023, respectively.[15–17] Estrogen receptor (ER) and progesterone receptor (PgR) were evaluated through IHC, while HER2 status was initially assessed by IHC and, in 2+ cases, presence of gene amplification by FISH. IHC stainings were performed using the automated platform Ventana BenchMark AutoStainer (Ventana Medical Systems, Tucson, AZ, USA) with the following primary antibodies: ER (CONFIRM anti-Estrogen Receptor (ER), Clone SP1, ref. 790-4324, prediluted), PR (CONFIRM anti-Progesterone Receptor (PR), Clone 1E2, ref. 790-2223, prediluted), HER2 (VENTANA anti-HER2/neu, clone 4B5, ref. 790-4493, prediluted), Glial Fibrillary Acidic Protein (GFAP, clone EP672Y, Cell Marque, ref. 258R-18, prediluted), Phospho-Stat3 (Tyr705) XP® (Cell Signaling, clone D3A7, ref. 9145, dilution 1:100). Glial Fibrillary Acid Protein (GFAP, clone EP6772Y, Cell Marque, ref. 258R-18, prediluied), Phospho-Stat3 (Tyr705) XP® (Cell Signaling, clone D3A7, ref. 9145, diluition 1:100).

For each IHC staining, standardized automated protocols were adopted: after a deparaffinization step in the oven at 60 °C overnight and with EZ Prep solution (Ventana Medical Systems, AZ, USA), antigen retrieval was performed using CC1 antigen retrieval buffer (pH 8.5, EDTA; Ventana Medical Systems, AZ, USA) at different temperatures and timing depending on primary antibody; the ultraView Universal DAB Detection Kit (Ventana Medical Systems, AZ, USA) detection system was used to detect ER, PgR, HER2, and pSTAT3 positivity through the chromogen 3, 3′-Diaminobenzidine (DAB), and nuclei were counterstained with Hematoxylin and Bluing reagent (Ventana Medical Systems, AZ, USA).

Nuclear pSTAT3 positivity in tumor cells BrM was evaluated semiquantitatively using the H-score to combine the staining intensity and the percentage of positive cells. Specifically, H-score was calculated by multiplying the staining intensity (0 for no staining, 1 for weak staining, 2 for moderate staining, and 3 for strong staining) by the percentage of cells showing that intensity and then summing the different results. Thus, the potential H-score ranged from 0 (no staining) to 300 (strong staining in all cells) and was assessed by two neuropathologists (L.B., P.C.) who were blinded of their scores.

For the scoring of pSTAT3 in reactive astrocytes, we have considered the area up to a maximum of 1 mm from the BrM border (Supplementary Figure 1). Astrocytes interspersed within the tumor mass were not evaluated.

To evaluate pSTAT3 nuclear positivity in peripheral reactive astrocytes, sections were simultaneously stained also for GFAP using the ultraView Universal Alkaline Phosphatase Red Detection Kit (Ventana Medical Systems, AZ, USA). Nuclear pSTAT3 expression was assessed by two independent neuropathologists (L.B., P.C.) using the semiquantitative score proposed by Priego et al.[11] as follows: score 3 was defined as moderate and diffuse expression, score 2 as moderate and focal expression or weak and diffuse expression, score 1 as weak and focal expression, while score 0 corresponded to absence of pSTAT3 nuclear positivity in reactive astrocytes (Supplementary Figures 2-A-E). In case of disagreement, the case was jointly discussed, and a consensus was reached.

Cell Culture

Human BrM cell lines have been previously described.[18–20] All cell lines were tested mycoplasma-free and validated by morphological analysis and their behavior in vitro and in vivo. MDA231-BrM were cultured in DMEM media supplemented with 10% fetal bovine serum (FBS), 2 mM L-Glutamine, 100 IU/ml penicillin/streptomycin, and 1 mg/ml amphotericin B. HCC1954-BrM were cultured in RPMI media supplemented with 10% FBS, 2 mM L-Glutamine, 100 IU/ml penicillin/streptomycin and 1 mg/ml amphotericin B.

Animal Studies

All animal experiments were performed in accordance with a protocol approved by the CNIO, Instituto de Salud Carlos III and Comunidad de Madrid Institutional Animal Care and Use Committee (PROEX135/19). Females athymic nu/nu (Harlan) 4-10 weeks of age were used. Housing and husbandry conditions are in accredited by AAALAC. Mice were SPF with microbiological and environmental parameters constantly monitored. Cancer cell colonization assays were performed by injecting 100 µl PBS into the left ventricle containing 100 000 cells (intracardiac injection) or 1 µl of PBS intracranially (right frontal cortex, 1.5 mm lateral and 1 mm caudal from bregma, depth of 2 mm) containing 40 000 cancer cells by using a gas-tight Hamilton syringe and a stereotactic apparatus (intracranial injection). The presence of the tumor in the brain was validated by bioluminescence (IVIS Spectrum PerkinElmer) and histological analysis.

Inmunofluorescence

For immunofluorescence, fixation with PFA 4% at 4 °C was applied to tissue prior to slicing of the brain by using a sliding microtome (80 µm slices) (Fisher). Brain slices were permeabilized with methanol for 20 min at –20 °C and then blocked in NGS 10%, BSA 2%, Triton 0.25% in PBS for 2 h at room temperature (RT). Primary antibodies: Anti-GFAP (1:1000, Millipore, ref. MAB360), Anti-GFP (1:1000, Aves Labs, ref. GFP-1020), and Anti-pSTAT3 (Tyr705) (1:100; Cell Signaling, ref. 9145) were incubated overnight at 4 °C in blocking solution and the following day for 30 min at RT. After washing in PBS-Triton 0.25%, secondary antibodies: Alexa-Fluor Anti-chicken488, Anti-mouse633, Anti-rabbit555 (1:300) were added in blocking solution and incubated for 2 h. After washing in PBS-Triton 0.25%, nuclei were stained with bisbenzimide (1 mg/ml; Sigma) for 7 min at RT. Images were acquired with a Leica SP5 up-right confocal microscope 20× objective (2.5 zoom).

Image acquisition and analysis

For histological analysis, images from whole slides were acquired with Thunder imaging system (Leica) 5× objective and analyzed with ImageJ software.

To analyze the percentage of lesions belonging to each size group, a categorization has been made regarding size as small, medium, and large, taking as reference the distribution of the total size of the lesions from the MDA231-BrM model.

Brain slice assays

Organotypic slice cultures from adult mouse brain with established brain metastasis (intracranial injection) were prepared as previously described.[11] Organotypic cultures included brains obtained 21 days after cancer cells inoculation when brain lesions are established. Brains were dissected in Hank's balanced salt solution (HBSS) supplemented with HEPES (pH 7.4, 2.5 mM), D-glucose (30 mM), $CaCl_2$ (1 mM), $MgCl_2$ (1 mM), $NaHCO_3$ (4 mM), and embedded in low-melting agarose (Lonza) preheated at 42 °C. The embedded brains were cut into 250 µm slices using a vibratome (Leica). Slices were divided at the hemisphere into two pieces. Brain slices were placed with flat spatulas on top of 0.8 µm pore membranes (Sigma Aldrich) floating on slice culture media (Dulbecco's modified Eagle's medium (DMEM), supplemented HBSS, FBS 5%, L-glutamine (1 mM), 100 IU/ml penicillin, 100 mg/ml streptomycin). BLI was acquired after generating brain slices (day 0) to confirm the presence of brain metastasis and 3 days after the addition of vehicle (DMSO) or silibinin (day 3). Growth rate was obtained by comparing fold increases between day 3 and day 0. DMSO/silibinin (100 µm, Sigma, ref. S0417) were added to the media at day 0.

Outcome Measures and Statistical Analysis

Baseline characteristics of patients included in the analysis were summarized using percentages and frequencies (*n*, %). The distribution of characteristics across patient subgroups was evaluated by Mann–Whitney U test for continuous variables and χ^2 test or Fisher exact test for categorical variables. The median i-PFS and 12-month i-PFS were measured from the date of surgery of BrM to the date of first local or distant BrM progression or death or last follow-up (censoring), whichever occurred first. Median i-PFS and 12-month i-PFS rates were reported as 95% exact binomial confidence intervals. A log rank test was performed to compare i-PFS of groups and a Cox regression model was performed to estimate hazard ratios. Statistical analyses were conducted using MedCalc® software v22.023. Immunofluorescence images were analyzed with ImageJ software. Data was analyzed using GraphPad Prism 8 software (GraphPad Software). For comparisons between 2 experimental groups in datasets that followed a normal distribution, an unpaired, two-tailed Student's *t*-test was used.

Results

Patients' characteristics

We identified 105 patients with BrM from BC diagnosed at the Pathology Unit of University of Turin ($n = 80$) and RENACER ($n = 25$) from January 2021 to April 2023. From 100/105 patients (95.2%) tumoral/peritumoral tissue was available for the purposes of this study. Baseline characteristics of the study cohort are described in Table 1. Female and white Europeans only have been included. Median age at BrM onset was 55 years (95% CI 50.72-58.27) with a median time to BrM development since the initial diagnosis of primary BC of 4.5 years (95% CI 3.0-5.27). BrM displayed a luminal subtype in 21/100 (21%) patients, a HER2-positive (HER2+) subtype in 37/100 (37%) and a triple-negative (TNBC) subtype in 42/100 (42%). Matched samples from primary BC were available in all patients: in 29/100 they displayed a luminal subtype (29%), in 32/100 (32%) a HER2-positive subtype, and in 39/100 (39%) a TNBC subtype. Concordance between molecular profile of matched primary BC and BrM was found in 79/100 (79%) patients, while the other 21/100 patients (21%) showed a molecular divergence. Overall, 10 luminal subtypes, 6TNBC, and 5 HER2-positive BC developed a molecular divergent BrM. Out of the 10 luminal BC, 6/10 BrM (60%) gained HER2 expression, while 4/10 BrM (40%) lost the ER/PgR expression. Of the 6TNBC, 3/6 (50%) BrM gained the ER/PgR expression and 3/6 (50%) gained HER2 expression. Last, of the 5 HER2 positive patients who displayed a molecular divergence, all BrM (100%) lost HER2 expression (Supplementary Table 1).

Thirty-four out of 100 patients (34%) and 15/100 (15%) had stable or progressive systemic disease, respectively, while 51/100 patients (51%) had absent systemic disease.

Eighteen out of 100 patients (18%) did not receive after surgery any adjuvant treatment, 21/100 (21%) received radiotherapy alone (18/21 SRS or conformal radiotherapy on surgical bed and 3/21 WBRT), 21/100 (21%) medical therapies alone (14/21 anti-HER2 agents, 6/21 cytotoxic chemotherapy, 1/21 CDK4-6 inhibitor), and 40/100 (40%) a combination of radiotherapy plus systemic treatment (SRS + cytotoxic chemotherapy in 13/40, SRS plus targeted therapy in 9/40, WBRT plus cytotoxic chemotherapy in 10/40, and WBRT plus targeted agents in 8/40). No patients received tucatinib or trastuzumab deruxtecan.

Median follow up of the whole cohort was 20.0 months (95% CI 14.34–24.82).

pSTAT3 is Expressed in the Majority of Reactive Astrocytes Surrounding Brain Metastases

The pSTAT3 expression was evaluated in both nuclear and cytoplasmatic compartments, and in both reactive astrocytes and BrM cells. pSTAT3 presented a preferential nuclear localization in both BrM cells and reactive astrocytes. A high pSTAT3 H-score in BrM cells (range 101-300) was found in 33/100 BrM samples (33%), while 67/100 BrM samples (67%) showed a low pSTAT3 H-score (0-100) (Supplementary Table 2A). High pSTAT3 expression (scores 2-3) in reactive astrocytes was detected in 57/100 BrM (57%), being score 3 in 23/57 (40%) and score 2 in 34/57 (59.6%). Low pSTAT3 expression (scores 0-1) was found in 43/100 BrM (43%): 12/43 (27.9%) were score 0 and 31/43 (72.1%) score 1. Overall, 88/100 (88%) BrM displayed a pSTAT3 positivity with a score ≥ 1 (Supplementary Table 2B).

pSTAT3 Expression in Reactive Astrocytes of Brain Metastases Differs According to Molecular Subtype, Number, and Site

pSTAT3 expression in reactive astrocytes significantly differed according to BrM molecular subtype: triple-negative

Table 1. Baseline patients' characteristics of the brain metastases cohort

	N	%
Gender		
F	100	100
M	0	0
Age at diagnosis of BC (y)		
Median	49	
<49	48	48.0
≥49	52	52.0
95% CI	45.0-54.0	
Primary BC molecular subtype		
Luminal	29	29.0
HER2-positive	32	32.0
TNBC	39	39.0
Surgery for primary BC		
Yes	93	93.0
No	7	7.0
Adjuvant radiotherapy for primary BC		
Yes	84	84.0
No	16	16.0
Adjuvant chemotherapy and/or targeted therapy for primary BC		
Yes	89	89.0
No	11	11.0
Adjuvant endocrine therapy for primary BC		
Yes	43	43.0
Tamoxifen	18/43	18.0
Aromatase inhibitor	25/43	25.0
No	57	57.0
Age at BrM diagnosis		
Median age	55	–
<55 years	49	49.0
≥55 years	51	51.0
95% CI	50.72-58.27	–
Time to develop BrM since initial diagnosis of primary BC		
Median	4.5	–
<5 years	50	50,0
≥5 years	50	50,0
95% CI	3.0-5.27	–
Number of BrM		
1	62	62.0
≥2	38	38.0
Site of BrM		
Supratentorial	54	54.0
Infratentorial	29	29.0
Both	17	17.0
KPS before BrM surgery		
Median	90	–
90-100	61	61,0
60-80	39	39,0

Table 1. Continued

	N	%
BrM molecular subtype		
Luminal	21	21,0
HER2+	37	37,0
Triple negative	42	42,0
Molecular divergence BrM/BC		
Yes	21	21,0
No	79	79,0
Extracrania/ disease at the time of BrM diagnosis		
Absent	51	51,0
Stable/controlled	15	15,0
Progressive	34	34,0
Treatment for BrM		
Surgery alone	18/100	18,0
RT alone	21/100	21,0
SRS	18/21	
WBRT	3/21	
Systemic therapy alone	21/100	21,0
Anti-HER2 agents	14/21	
Cytotoxic CT	6/21	
CDK 4/6 inhibitor	1/21	
Combination of RT plus systemic therapy	40/100	40,0
SRS plus cytotoxic CT	13/40	
SRS plus targeted therapy	9/40	
WBRT plus cytotoxic CT	10/40	
WBRT plus targeted therapy	8/40	
Type of drugs following BrM surgery		
Anti-HER2 agents	30/61	30,0
Capecitabine + lapatinib	16/61	16,0
Capecitabine + neratinib	4/61	4,0
T-DM1	10/61	10,0
CDK4/6 inhibitors	1/61	1,0
PARP inhibitors	2/61	2,0
Cytotoxic chemotherapy	28/61	28,0
Capecitabine	22/61	22,0
Eribulin	4/61	4,0
Vinorelbine + paclitaxel	2/61	2,0
None	39	39,0
Adjuvant endocrine therapy following BrM surgery		
Yes	32	32,0
Tamoxifen	3/32	3,0
Aromatase inhibitor	29/32	29,0
None	68	68,0
Intracranial recurrence following surgery alone	18	18,0
Yes	7/18	42,1
No	11/18	57,9
Intracranial recurrence following surgery plus adjuvant therapies		
Yes	54	54.0
No	46	46.0

Table 1. Continued

	N	%
Type of intracranial recurrence (*N* = 54)		
Local	20	37.0
Distant	25	46.3
Local plus distant	9	16.7

BC, breast cancer; BrM, brain metastasis; CDK 4-6, cyclin dependent kinases 4-6; CI, confidence interval; HER2, human epidermal growth factor receptor 2; KPS, Karnofsky performance status; F, female; M, male; PARP, poly-ADP ribose polymerase; RT, radiotherapy; SRS, stereotactic radiosurgery; STAT3, signal transducer and activator of transcription 3; T-DM1, trastuzumab emtansine; WBRT, whole-brain radiotherapy.

BrM showed higher pSTAT3 expression (34/42, 80.9%) in comparison to HER2-positive BrM (16/37, 43.2%) and luminal BrM (7/21, 33.3%) (*P* .002; Supplementary Figure 6A).

When BrM were multiple (≥2), the single lesion that was examined displayed a higher pSTAT3 expression in reactive astrocytes (high pSTAT3 28/38, 73.7% vs low pSTAT3 10/28, 26.3%) in comparison with single BrM where pSTAT3 expression was almost equally distributed (low pSTAT3 33/62; 53.2%; high pSTAT3 29/62; 46.8%) (*P* = .0087; Supplementary Figure 6B). Multiple lesions in both supratentorial and infratentorial compartments expressed higher level of pSTAT3 in reactive astrocytes (15/17, 88.2%) as compared with lesions in the sole supratentorial (30/54, 55.5%) or infratentorial compartment (12/29, 41.4%) (*P* = .0078; Supplementary Figure 6C).

pSTAT3 expression in reactive astrocytes was not influenced by factors, such as age at the time of diagnosis of BrM, time to development of BrM, and systemic disease status (Supplementary Table 3).

Moreover, a high pSTAT3 expression in reactive astrocytes prevailed in BrM with the same molecular profile with primary tumor (49/79, 62.0%), while low pSTAT3 expression prevailed when molecular divergence occurred between BrM and matched primary BC (13/21, 61.9%) (*P* = 0.0501) (Supplementary Table 3, Supplementary Figure 7).

Last, pSTAT3 H-score of BrM tumor cells did not show any correlation with clinical or molecular factors, with the exception of KPS (Supplementary Table 4).

pSTAT3 Expression in Reactive Astrocytes of Experimental Brain Metastases Differs According to Molecular Subtype

To explore whether our findings are replicated in preclinical models of BrM, we used two different breast cancer brain metastatic cell lines for specific subtypes: MDA231-BrM cells for triple negative breast cancer brain metastasis and HCC1954-BrM cells for HER2-positive breast cancer brain metastasis.[21]

We injected intracardially adult mice to obtain established brain metastases (Figure 1A). Notably, the MDA231-BrM cells exhibited higher tumorigenic potential in the brain (Supplementary Figure 8A-D). Following the induction of brain metastases using both models, a more aggressive growth pattern was observed in the triple-negative breast cancer brain metastasis model, characterized by a greater number of lesions with bigger tumor size (Supplementary Figure 8B-D).

To test if the molecular activation pattern of STAT3 in metastasis-associated astrocytes differs between the two different subtypes, we performed pSTAT3 staining by immunofluorescence in established brain metastasis lesions classified as medium size (Supplementary Figure 8D) for both models (Figure 1A). Immunofluorescence analysis of reactive astrocytes located in the peritumoral area, confirmed differential pSTAT3 enrichment in established lesions of MDA231-BrM and HCC1954-BrM cells (Figure 1A-B). Remarkably, positive pSTAT3 expression in GFAP + astrocytes was detected in 50% of the total reactive astrocytes surrounding the tumor lesion in the triple negative breast cancer brain metastasis model (MDA231-BrM) compared with a milder activation, with only 13% of reactive astrocytes activating STAT3, in the HER2-positive model (HCC1954-BrM) (*P* = .0001) (Figure 1A-C).

Although genetic validation would be required, this finding, together with the observed histological differences showing fewer large lesions in the HCC1954-BrM model (Supplementary Figure 8D), may suggest a dependence on astrocytic STAT3 activity for the formation of large metastases.

Response of Experimental Brain Metastases to STAT3 Inhibition is Shaped by the Breast Cancer Subtype

The degree of pSTAT3 activation in reactive astrocytes observed in experimental brain metastasis representing the two breast cancer subtypes aligned with patient data, which is of notable interest to design specific genetic and pharmacological strategies targeting microenvironment-derived STAT3-dependent survival mechanisms.[11,13] Therefore, we conducted an initial analysis of the sensitivity of both models to STAT3 inhibition, using the STAT3 inhibitor silibinin previously reported to be effective in other models of brain metastasis and in human patients.[22,23] Although both cell lines showed some degree of sensitivity to STAT3 inhibition in vitro (Supplementary Figure 9A-B), ex vivo experiments using established metastases—where STAT3 activation is restricted to the microenvironment—showed that only the MDA231-BrM model exhibited a significant reduction in proliferation when treated with silibinin (Figure 2A-C).

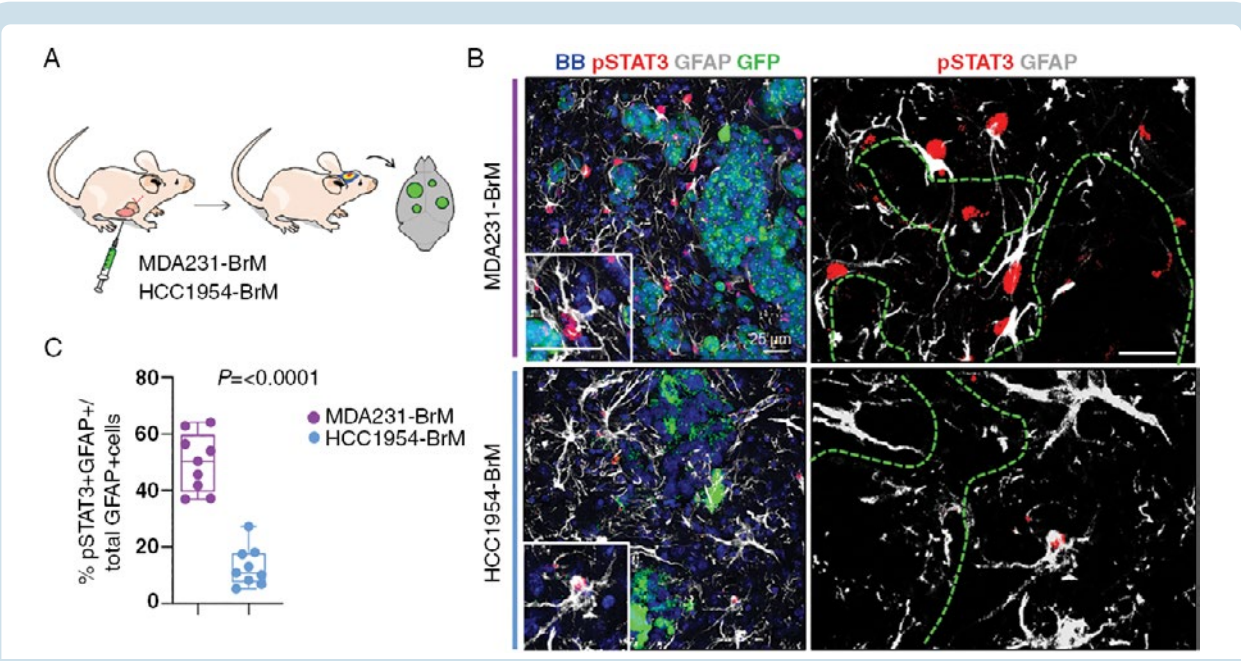

Figure 1. pSTAT3 expression in reactive astrocytes of experimental brain metastases differs according to molecular subtype. (A) Schema of the experimental design. Mice were intracardially injected with MDA231-BrM and HCC1954-BrM cells, and after established brain metastasis was formed, their brains were processed for further analysis of the tumor microenvironment. (B) Representative images of brain metastasis lesions quantified in (C). Dotted line indicates metastatic lesions in the magnifications. BB: bisbenzimide for nuclei staining. (C) Graphical representation of the percentage of pSTAT3 + GFAP + cells among all the GFAP + cells. Values are shown in box-and-whisker plots where every dot is a different lesion. Three different brains (3 mice) and three lesions per condition are quantified. The *P* value is calculated using the two-tailed *t*-test. Scale bar and magnification: 25 µm.

Given the differences in tumor growth patterns observed in the two models (Supplementary Figures 8A-D and 9C), we aimed to determine whether MDA231-BrM lesions equivalent to those found in HCC1954-BrM brain metastases, were also sensitive to STAT3 inhibition. To this end, we performed additional ex vivo cultures using brain slices with established MDA231-BrM metastases showing similar bioluminescence signal compared to the HCC1954-BrM model (Supplementary Figure 9D). Our results confirm that both big and medium size MDA231-BrM brain metastatic lesions are sensitive to STAT3 inhibition (Figure 2A-C, Supplementary Figure 9D).

In conclusion, triple-negative breast cancer brain metastasis and HER2-positive breast cancer brain metastasis experimental models differ in their sensitivity to STAT3 inhibition, with the triple negative model exhibiting a consistent therapeutic response.

Correlations between Patterns of pSTAT3 Expression on Reactive Astrocytes of Brain Metastases and Risk of Intracranial Recurrence and i-PFS

At the time of the analysis (November 2024), 54/100 patients (54.0%) recurred intracranially with a coexistence of extracranial progression in 42/100 (42.0%).

Twenty out of 54 patients (37.0%) had a local intracranial progression, 25/54 (46.3%) a distant intracranial progression, and 9/54 (16.7%) both a local and distant intracranial progression (Table 1). Four out of 54 patients (7.4%) developed a leptomeningeal spread (2 from HER2-positive BrM and 2 from triple-negative BrM) in association with supratentorial (3/4) or infratentorial (1/4) progression.

Intracranial recurrence after BrM surgery prevailed in patients with high pSTAT3 expression in reactive astrocytes (high pSTAT3 36/54, 66.7% vs low pSTAT3 18/54, 33.3%), while low pSTAT3 expression prevailed in patients who did not recur intracranially (low pSTAT3 25/46, 54.3% vs high pSTAT3 21/24, 45.7%) ($P = .0353$) (Supplementary Table 3, Supplementary Figure 10). All patients who developed leptomeningeal spread displayed a high pSTAT3 expression (3/4 score 2 and 1/4 score 3).

Median i-PFS of the whole cohort was 14 months (95% CI 12-29). Patients with high pSTAT3 expression in reactive astrocytes showed a shorter median i-PFS (9 months, 95% CI 7-12) as compared with patients with low pSTAT3 expression (28 months, 95% CI 21-35; HR 2.96, 95CI% 1.67-5.24; $P = .0002$) (Supplementary Table 2B, Figure 3A). Likewise, 12-month i-PFS was shorter in high pSTAT3 BrM (36.0%, SD ± 7.03) in comparison to low pSTAT3 BrM (82%, SD ± 6.18). After multivariable analysis, pSTAT3 expression in reactive astrocytes (HR 2.35; 95% CI 1.23-4.52; $P = .0138$) retained the statistical significance in addition to molecular subtype (Table 2). Conversely, H-score of BrM tumor cells and status of extracranial disease were not associated with i-PFS in both univariable and multivariable analysis (Table 2).

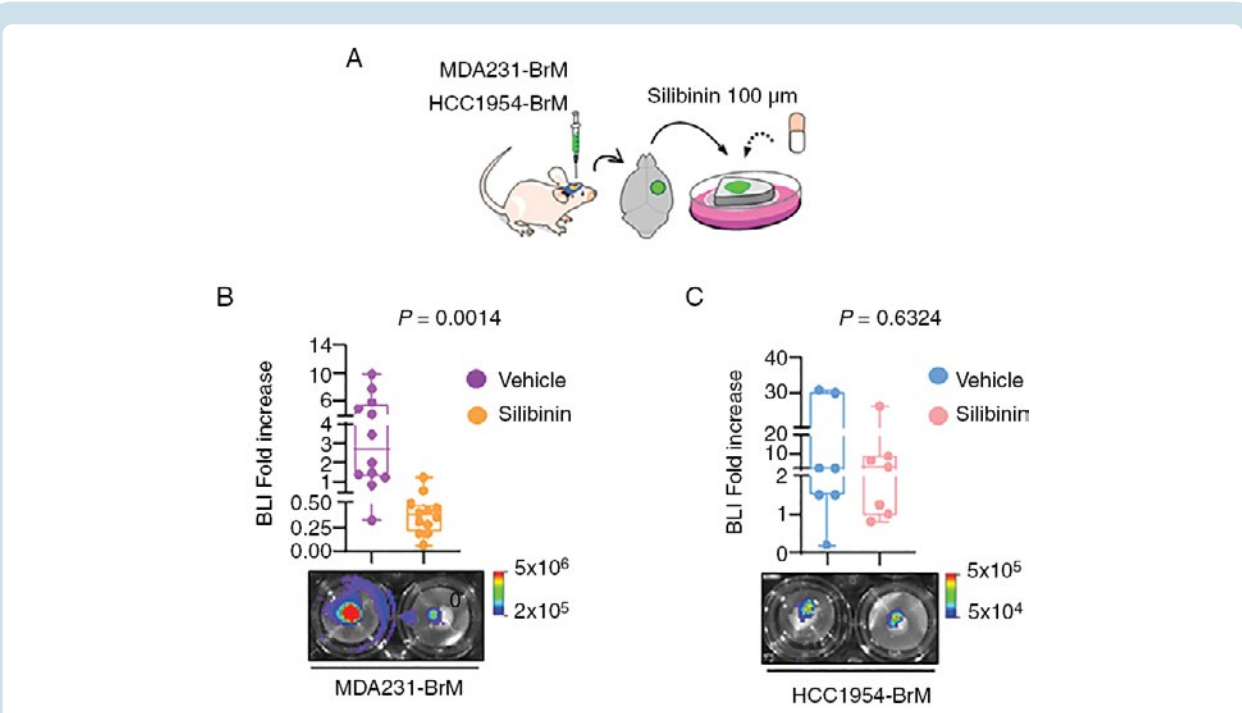

Figure 2. Response to STAT3 inhibition varies according to the molecular subtype in experimental brain metastasis from breast cancer. (A) Schema of the experimental design. Mice were intracranially injected with MDA231-BrM and HCC1954-BrM cells, and after brain metastases are established formed, their brains were processed for brain slices assays. (B, C) Quantification of the BLI signal emitted by MDA231-BrM cells (A) and HCC1954-BrM cells (B) in each brain slice of established tumor normalized by the initial value obtained at time 0, before the addition of vehicle (DMSO) or sibilibin (100 µm). Values are shown in box-and-whisker plots in which every dot represents a different organotypic culture and the line in the box corresponds to the median. Whiskers go from minimum to maximum values ($n = 12$ independent organotypic cultures in (A) and $n = 7$ independent organotypic cultures in (B). Quantification is accompanied by representative images of wells containing brain organotypic cultures with established metastases grown ex vivo for 72 h. The image shows the BLI intensity in each condition for each brain slice. *P* values were calculated using the two-tailed *t*-test.

Intracranial PFS across molecular subtypes is reported in Supplementary Table 5. Among patients with triple-negative BrM high pSTAT3 expression was significantly associated with shorter median i-PFS and 12-month i-PFS (7 months and 12.7%) as compared to low pSTAT3 expression (21 months and 85.3%) (HR 5.01, CI 95% 2.04-12.27, $P = .0004$) (Table 3, Figure 3B). Among patients with luminal and HER2-positive BrM high pSTAT3 expression was associated with shorter median i-PFS (16 months and 11 months) and 12-month i-PFS (75% and 50%) as compared with low pSTAT3 expression (median i-PFS 49 months and 30 months; 12-month i-PFS 85.7% and 71.2%), however, the difference did not reach statistical significance (Table 3, Figure 3C-D).

Interestingly, the presence of a higher pSTAT3 expression influenced PFS both in case of molecular divergence (high pSTAT3 with a median i-PFS 12.0 months, and 12-month i-PFS 50.0%, HR 7.14 vs low pSTAT3 median i-PFS 28.0 months, and 12-month i-PFS 87.5%, HR 1.0, $P = .0331$) and in case of molecular concordance (high pSTAT3 i-PFS 8.0 months and 12-month i-PFS 33.4% HR 2.53 vs low pSTAT3 i-PFS not reached and 12-month i-PFS 78% HR 1.0, $P = .0041$). Of note, the subgroup with low-pSTAT3 expression and concordant molecular profile between BrM/BC had a longer i-PFS (i-PFS not reached; 12-month i-PFS 78.0%) (Supplementary Table 6).

Discussion

The importance of the expression of STAT3 in reactive astrocytes surrounding BrM in promoting tumor growth and invasion was demonstrated in preclinical models.[11,14] Also, a prognostic value of STAT3 expression was suggested in a small cohort of patients with BrM from miscellaneous solid tumors.[11]

In this paper, we focused our attention on a large and homogeneous cohort of patients with completely resected BrM from BC, and analyzed the correlations between STAT3 expression in reactive astrocytes and clinical and molecular factors as well as the influence on patterns of tumor recurrence in the brain and intracranial PFS. Moreover, we wanted to see whether the different distribution of STAT3 across molecular subtypes in the human material could be observed in experimental models of BrM from breast cancer as well.

It must be stated that in the experiments described in this paper we did not investigate the functional role of peritumoral astrocyte STAT3 activation on tumor growth/progression, as it was assumed based on our previous work.[11]

Most of results of our study are new, and have not been previously published.

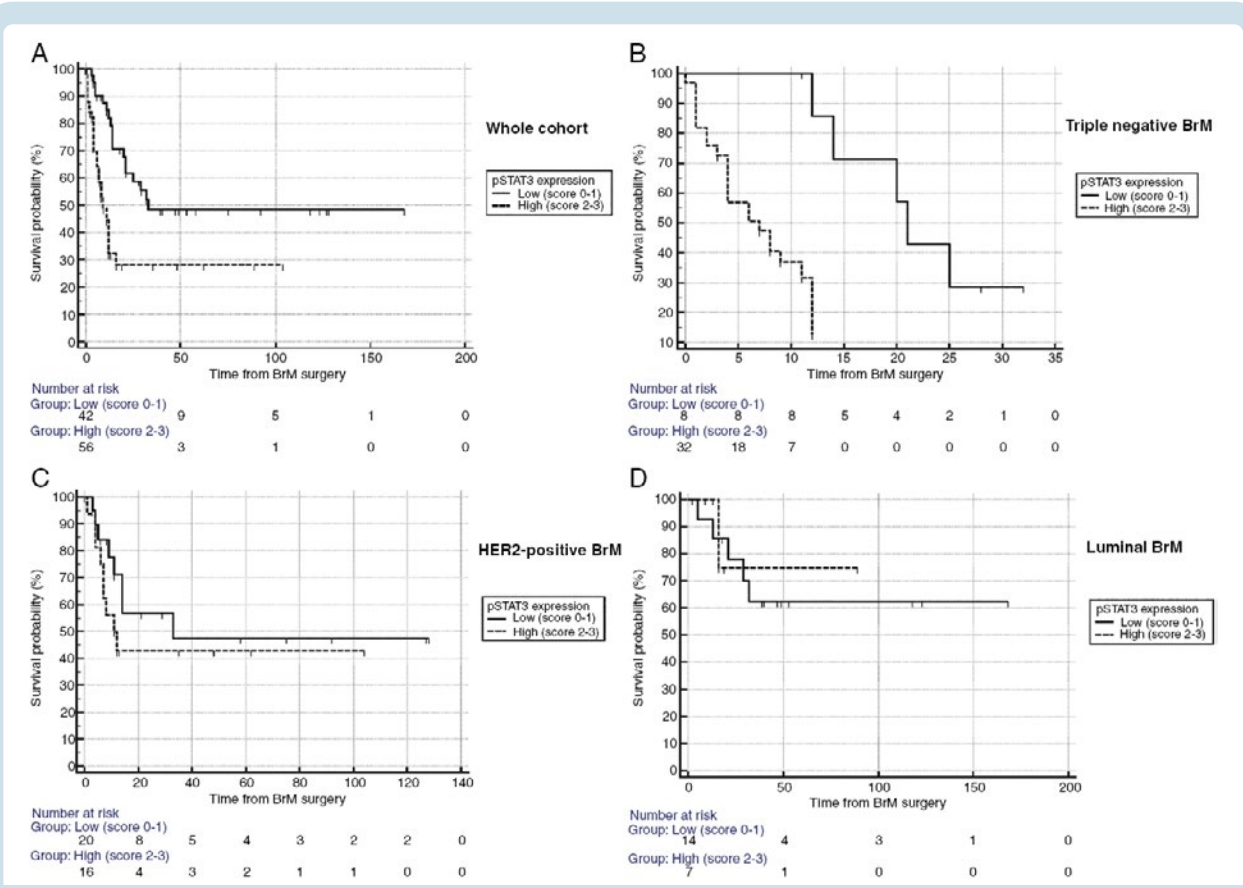

Figure 3. i-PFS according to patterns of pSTAT3 expression in the whole cohort (A) and molecular subtypes (B-D).

First, a significantly higher STAT3 expression was found in triple-negative BrM in comparison to HER2-positive and luminal BrM. These findings were confirmed in the experimental models that we investigated, and reinforce the concept that experimental models could be useful to test anti-STAT3 strategies before moving to clinical setting. Moreover, multiple BrM may display some heterogeneity in the amount of STAT3 expression as compared to single metastasis: this finding should be verified through the resection and analysis of more than one lesion in the same patients.

Patterns of tumor recurrence in the brain after BrM surgery and intracranial PFS of our cohort are similar to those of other series.[3]

In our cohort intracranial recurrence significantly prevailed in patients with high STAT3 expression as compared to those with low STAT3 expression, in whom an extracranial progression prevailed. Moreover, patients, who developed leptomeningeal spread, had a high STAT3 expression, and original BrM were located in the supratentorial compartment and underwent en-block resection.

The prognostic importance of STAT3 expression in reactive astrocytes of BrM in terms of intracranial PFS was confirmed by the multivariable analysis including the most relevant clinical factors.

An interesting finding of our study is that intracranial PFS had a prognostic value that differed according to molecular subtype being a high STAT3 expression significantly associated with shorter median and 12-month intracranial PFS in triple-negative patients only. The strength of this result is confirmed by the fact that within each molecular subtype patients with high and low STAT3 expression were balanced for clinical factors of prognostic importance (Supplementary Table 7).

Some studies suggested STAT3 expression in primary BC cells as a negative prognostic marker and target of therapy, particularly in triple-negative subtypes.[24,25] We did not find such a correlation in our study on BrM: this could be partly due to our criteria of nuclear staining and scoring, but could also suggest that the expression of STAT3 in cancer cells of BrM is less relevant in terms of prognosis as compared to cells of primary tumors.

Based on the results of this study, we suggest that the expression of STAT3 in reactive astrocytes surrounding BrM should be considered as a biomarker of prognostic significance: in this regard, an evaluation of the association with OS in future studies is needed. We could not explore this hypothesis due to the short follow-up with a limited number of death events. However, due to the significant correlation with intracranial PFS, we suggest a closer MRI monitoring after surgical resection of a single BrM in patients whose lesions display a high STAT3 expression (in particular triple negative patients).

STAT3 may be also a target of therapy. Danker et al.[14] reported in experimental models that STAT3 inhibition via

Table 2. Correlations of clinical and molecular factors with i-PFS: univariate and multivariable analysis

	Univariate analysis		Multivariable analysis	
Factors	HR (CI 95%)	*P* value	HR adj (CI 95%)	*P* value
Age at diagnosis of BrM (y)				
<55 years (*n* = 49)	1	.1896	1	.2419
≥55 years (*n* = 51)	1.44 (0.83-2.50)		0.72 (0.42-1.25)	
BrM molecular subtypes				
Luminal (*N* = 21)	1		1	
HER2-positive (*N* = 37)	2.29 (1.21-4.36)		2.21 (1.55-3.54)	
Triple negative (*N* = 42)	5.32 (2.69-10.49)	**<.0001**	3.02 (1.48-4.57)	**.0002**
Number of BrM				
1 (*N* = 62)	1		1	
≥2 (*N* = 38)	1.09 (0.61-1.93)	0.08194	0.83 (0.46-1.48)	.5339
KPS before BrM surgery				
90-100 (*N* = 61)	1	0.2519	1	
60 - 80 (*N* = 39)	1.39 (0.79-2.43)		0.79 (0.44-1.42)	.4366
pSTAT3 H-score in BrM cells				
Low (0-100) (*N* = 67)	1	.2129	1	.7549
High (101-300) (*N* = 33)	1.45 (0.81-2.58)		0.91 (0.49-1.66)	
pSTAT3 expression in reactive astrocytes				
Low (scores 0-1) (*N* = 43)	1	**.0002**	1	**.0138**
High (scores 2-3) (*N* = 57)	2.96 (1.67-5.24)		2.35 (1.23-4.52)	
Extracranial disease at the time of BrM diagnosis				
Absent (*N* = 51)	1		1	
Stable/controlled (*N* = 15)	0.56 (0.27-1.15)	.3480	0.95 (0.69-1.30)	.7514
Progressive (*N* = 34)	1.22 (0.52-2.03)		1.89 (0.43-2.13)	
Adjuvant treatment for BrM surgery				
Yes (*N* = 88)	1	.6634	1	.3294
No (*N* = 18)	1.17 (0.57-2.43)		1.49 (0.67-3.34)	

BrM: brain metastasis; CI: confidence interval; HER2: human epidermal growth factor receptor 2; HR: odds ratio; KPS: Karnofsky performance status; STAT3: signal transducer and activator of transcription 3.

the specific STAT3 inhibitor silibinin or genetic ablation interferes with the growth of highly invasive BrM. In this study, we showed that experimental BC brain metastasis models exhibit subtype-dependent response to STAT3 inhibition with silibinin with promising results in the triple-negative model. Efficacy of silibinin has been previously reported in a small series of patients with advanced inoperable BrM from NSCLC.[22] Silibinin is under investigation in a multicenter randomized phase 2 trial (SILMET trial, NCT05689619), that evaluates its efficacy in preventing local recurrence of a single BrM from BC and NSCLC after gross total resection. Other novel therapeutic strategies to target STAT3 are under investigation.[26–28] Overall, targeting STAT3 is particularly attractive for patients with triple-negative BC as targeted therapies or immunotherapy are of limited value.

Identifying the source of STAT3 activation in astrocytes across patients and different experimental models is of interest for newer therapeutic strategies. Our previous studies identified STAT3 activators in reactive astrocytes during advanced disease stages in experimental models, such as IL-6, EGF, PDGF or distinct cytokines.[11,13] We observed different expression patterns of STAT3-inducing factors among the BC brain metastatic cell lines: the MDA231-BrM line expresses higher levels of EGF, MIF, CNTF, and IL-6 compared to HCC1954-BrM, suggesting a greater capacity to activate STAT3 signaling in astrocytes.[11]

This study has several limitations. First, the sample size is limited for a meaningful statistical analysis within each molecular subgroup: future studies should validate our findings in larger independent cohorts of patients with BrM from BC. Second, pSTAT3 normalization by tumor area or volume was not feasible in such a retrospective study with archival histopathology slides. Third, activation of peritumoral astrocytic STAT3 in clinical specimens may have a prognostic value, but whether it has the same functional relevance as observed in experimental models remains to be proven. Moreover, we have not analyzed the

Table 3. Correlations between patterns of pSTAT3 expression in reactive astrocytes of brain metastases according to molecular subtype and i-PFS

BrM subtype	pSTAT3 expression	Median intracranial PFS months (95% CI)	12-month intracranial PFS % (± SD)	HR (95% CI)	*P* value
Luminal	Low (scores 0-1)	49.0 (29.04- 118.0)	85.7 (± 9.35)	1	
	High (scores 2-3)	16.0 (9.55-18.58)	75.0 (± 21.7)	1.12 (0.13-9.48)	.912
HER2-positive	Low (scores 0-1)	30.0 (11.0-33.0)	71.2 (± 11.0)	1	
	High (scores 2-3)	11.0 (6.0-12.0)	50.0 (± 12.5)	1.59 (0.59-4.27)	.350
Triple negative	Low (scores 0-1)	21.0 (12.0- 25.0)	85.3 (± 13.2)	1	
	High (scores 2-3)	7.0 (4.0-11.0)	12.7 (± 7.8)	5.01 (2.04-12.27)	**.0004**

BrM: brain metastases; CI: confidence interval; HR: hazard ratio; HER2: human epidermal growth factor receptor 2; PFS: progression-free survival; SD: standard deviation; STAT3: signal transducer and activator of transcription 3.

immune cell populations, that could play a role in the development of BrM and in predicting OS of the BC molecular subgroups.[29]

Overall, the results of this study apply only to the small subgroup of patients with BrM who underwent a surgical resection and have a better outcome, and cannot be extrapolated to the whole group of BrM, in whom the expression of STAT3 is unknown. In this regard, the need to determine STAT3 expression could represent an argument, in addition to the well-known risk of molecular divergence, in favor for extending surgical indications to patients with small or asymptomatic BrM before any treatment.

We also acknowledge the limitations associated with the use of a single cell line for triple negative BC brain metastasis and HER2-positive BC brain metastasis and underscore the importance of expanding the analysis to additional models representative of the subtypes under investigation.

In summary, this study indicates that STAT3 expression prevails in reactive astrocytes surrounding triple-negative BrM in comparison to HER2-positive BrM, and this finding mirrors what was observed in animal models. Moreover, a high STAT3 expression is correlated with higher risk of intracranial recurrence and shorter intracranial progression-free survival, and this is particularly evident for patients with triple-negative BrM.

Supplementary material

Supplementary material is available online at *Neuro-Oncology* (https://academic.oup.com/neuro-oncology).

Keywords

brain metastases | breast cancer | reactive astrocytes | STAT3 expression | silibinin

Conflict of interest statement, **All the authors declare no conflict of interest.**

Funding

This work was supported by ERC CoG [864759 to M.V.], ERANET-TRANSCAN-3 (TRANSCAN2021-2023) [M.V.] with funds from Instituto de Salud Carlos III/NextGenerationEU/PRTR (AC20/00114) and FC AECC (TRNSC213878VALI), AECC Coordinados [PRYCO234528VALI, M.V.], AECC postdoctoral fellowship (POSTD19016PRIE) [N.P.], ERANET-TRANSCAN-3 (TRANSCAN 2021-2023) with funds from the Italian Ministry of University and Research (D63C23000040001) [L.B.].

Notes

RENACER: Manuel Valiente[1], Patricia Baena[1], Diana Retana[1], Virginia Calvo[1], Cecilia Sobrino[2], Daniel Alba-Olano[2], Carmen Ortega-Sabater[2], Inmaculada Almenara-Gonzalez[2], Nuria Ajenjo[2], Maria-Jesus Artiga[2], Eva Ortega-Paino[2], Juan Delgado-Fernández[3], Ángel Pérez-Nuñez[3-5], Aurelio Hernández-Laín[6], Óscar Toldos-González[6], Ricardo Gargini[6], Denisse Alcivar[6]

[1]Brain Metastasis Group, Spanish National Cancer Research Centre (CNIO), Madrid, Spain

[2]Biobank, Spanish National Cancer Research Centre (CNIO), Madrid, Spain

[3]Neurosurgery, Department of Neurosurgery, Hospital Universitario 12 de Octubre, Madrid, Spain

[4]Department of Surgery, Faculty of Medicine, Universidad Complutense de Madrid, Madrid, Spain

[5]Health Research Institute Hospital 12 de Octubre, Madrid, Spain

[6]Anatomopathology Department, Hospital Universitario 12 de Octubre, Madrid, Spain

Data availability

Any requests for raw and analyzed data should be addressed to the corresponding author Alessia Pellerino. Patient-related data in the paper were generated as part of a retrospective study and are subject to patient confidentiality. Any data and materials (eg tissue samples or clinical data) that can be shared will need approval from the institutional review board and a Material Transfer Agreement in place. All data shared will be de-identified.

Authorship

Study design: A.P., R.S., M.V.
Data acquisition: A.P., N.P., L.B., A.A.R., L.M., F.B., A.B., G.M., M.M., D.G., J.B.B., P.C.
Data analysis and interpretation: A.P., N.P., R.S., R.R.
Drafting the manuscript: A.P., N.P.
Final approval of the manuscript: All Authors

Affiliations

Division of Neuro-Oncology, Department of Neuroscience "Rita Levi Montalcini," University and City of Health and Science Hospital, Turin, Italy (A.P., F.B., R.R.); Spanish National Cancer Research Centre (CNIO), Madrid, Spain (N.P., M.V.); Pathology Unit, Department of Medical Sciences, University and City of Health and Science Hospital, Turin, Italy (L.B., A.A.R., L.M., P.C.); Breast Medical Oncology, Department of Oncology, City of Health and Science Hospital, Turin, Italy (A.B., G.M., M.M.); Neurosurgery Unit, Department of Neuroscience "Rita Levi Montalcini," University and City of Health and Science Hospital, Turin, Italy (D.G.); Department of Medical Oncology, Catalan Institute of Oncology, Doctor Josep Trueta University Hospital, Girona, Spain (J.B.-B.); Precision Oncology Group (OncoGIR-Pro), Girona Biomedical Research Institute (IDIBGI-CERCA), Salt, Spain (J.B.-B.); Department of Medical Sciences, Medical School, University of Girona, Girona, Spain (J.B.-B.); Biobank, Spanish National Cancer Research Centre (CNIO), Madrid, Spain (RENACER); Candiolo Cancer Institute, FPO-IRCCS, Candiolo (Turin), Italy (R.S.)

References

1. Kuksis M, Gao Y, Tran W, et al. The incidence of brain metastases among patients with metastatic breast cancer: a systematic review and meta-analysis. *Neuro Oncol.* 2021;23(6):894–904.
2. Darlix A, Louvel G, Fraisse J, et al. Impact of breast cancer molecular subtypes on the incidence, kinetics and prognosis of central nervous system metastases in a large multicentre real-life cohort. *Br J Cancer.* 2019;121(12):991–1000.
3. Pasquier D, Darlix A, Louvel G, et al. Treatment and outcomes in patients with central nervous system metastases from breast cancer in the real-life ESME MBC cohort. *Eur J Cancer.* 2020;125:22–30.
4. Müller V, Bartsch R, Lin NU, et al. Epidemiology, clinical outcomes, and unmet needs of patients with human epidermal growth factor receptor 2-positive breast cancer and brain metastases: A systematic literature review. *Cancer Treat Rev.* 2023;115:102527.
5. Poletes C, Amanirad B, Santiago AT, et al. The incidence of brain metastases in breast cancer according to molecular subtype and stage: a 10-year single institution analysis. *J Neurooncol.* 2024;169(1):119–127.
6. Arvold ND, Oh KS, Niemierko A, et al. Brain metastases after breast-conserving therapy and systemic therapy: incidence and characteristics by biologic subtype. *Breast Cancer Res Treat.* 2012;136(1):153–160.
7. Corti C, Antonarelli G, Criscitiello C, et al. Targeting brain metastases in breast cancer. *Cancer Treat Rev.* 2022;103:102324.
8. Ramakrishna N, Anders CK, Lin NU, et al. Management of advanced human epidermal growth factor receptor 2-positive breast cancer and brain metastases: ASCO guideline update. *J Clin Oncol.* 2022;40(23):2636–2655.
9. Boire A, Brastianos PK, Garzia L, Valiente M. Brain metastasis. *Nat Rev Cancer.* 2020;20(1):4–11.
10. Álvaro-Espinosa L, de Pablos-Aragoneses A, Valiente M, Priego N. Brain microenvironment heterogeneity: potential value for brain tumors. *Front Oncol.* 2021;11:714428.
11. Priego N, Zhu L, Monteiro C, et al. STAT3 labels a subpopulation of reactive astrocytes required for brain metastasis. *Nat Med.* 2018;24(7):1024–1035.
12. Wang T, Niu G, Kortylewski M, et al. Regulation of the innate and adaptive immune responses by Stat-3 signaling in tumor cells. *Nat Med.* 2004;10(1):48–54.
13. Priego N, de Pablos-Aragoneses A, Perea-García M, et al. TIMP1 mediates astrocyte-dependent local immunosuppression in brain metastasis acting on infiltrating CD8+ T cells. *Cancer Discov* 2025;15(1):179–201.
14. Dankner M, Maritan SM, Priego N, et al. Invasive growth of brain metastases is linked to CHI3L1 release from pSTAT3-positive astrocytes. *Neuro Oncol.* 2024;26(6):1052–1066.
15. Allison KH, Hammond MEH, Dowsett M, et al. Estrogen and progesterone receptor testing in breast cancer: ASCO/CAP guideline update. *J Clin Oncol.* 2020;38(12):1346–1366.
16. Wolff AC, Hammond MEH, Allison KH, et al. Human epidermal growth factor receptor 2 testing in breast cancer: American Society of Clinical Oncology/College of American Pathologists Clinical Practice Guideline Focused Update. *J Clin Oncol.* 2018;36(20):2105–2122.
17. Wolff AC, Somerfield MR, Dowsett M, et al. Human epidermal growth factor receptor 2 testing in breast cancer: ASCO-College of American Pathologists Guideline Update. *J Clin Oncol.* 2023;41(22):3867–3872.
18. Bos PD, Zhang XH, Nadal C, et al. Genes that mediate breast cancer metastasis to the brain. *Nature.* 2009;459(7249):1005–1009.
19. Kim MY, Oskarsson T, Acharyya S, et al. Tumor self-seeding by circulating cancer cells. *Cell.* 2009;139(7):1315–1326.
20. Gazdar AF, Kurvari V, Virmani A, et al. Characterization of paired tumor and non-tumor cell lines established from patients with breast cancer. *Int J Cancer.* 1998;78(6):766–774.
21. Valiente M, Van Swearingen AED, Anders CK, et al. Brain metastasis cell lines panel: a public resource of organotropic cell lines. *Cancer Res.* 2020;80(20):4314–4323.
22. Bosch-Barrera J, Sais E, Cañete N, et al. Response of brain metastasis from lung cancer patients to an oral nutraceutical product containing silibinin. *Oncotarget.* 2016;7(22):32006–32014.
23. Verdura S, Cuyàs E, Llorach-Parés L, et al. Silibinin is a direct inhibitor of STAT3. *Food Chem Toxicol.* 2018;116(Pt B):161–172.
24. Stover DG, Gil Del Alcazar CR, Brock J, et al. Phase II study of ruxolitinib, a selective JAK1/2 inhibitor, in patients with metastatic triple-negative breast cancer. *NPJ Breast Cancer.* 2018;4:10.
25. Lynce F, Stevens LE, Li Z, et al. TBCRC 039: a phase II study of preoperative ruxolitinib with or without paclitaxel for triple-negative inflammatory breast cancer. *Breast Cancer Res.* 2024;26(1):20.
26. Hong D, Kurzrock R, Kim Y, et al. AZD9150, a next-generation antisense oligonucleotide inhibitor of STAT3 with early evidence of clinical activity in lymphoma and lung cancer. *Sci Transl Med.* 2015;7(314):314ra185.
27. Bai L, Zhou H, Xu R, et al. A potent and selective small-molecule degrader of STAT3 achieves complete tumor regression in vivo. *Cancer Cell.* 2019;36(5):498–511.e17.
28. Zhou H, Bai L, Xu R, et al. Structure-based discovery of SD-36 as a potent, selective, and efficacious PROTAC degrader of STAT3 protein. *J Med Chem.* 2019;62(24):11280–11300.
29. Griguolo G, Tosi A, Dieci MV, et al. A comprehensive profiling of the immune microenvironment of breast cancer brain metastases. *Neuro Oncol.* 2022;24(12):2146–2158.